Solving Multidimensional Continuum Mechanics Problems on Unstructured Lagrange Meshes

Sokolov S.S.

Russian Federal Nuclear Center – VNIIEF
37 Mira pr., Sarov, Nizhniy Novgorod region, Russia

The paper discusses the effort carried out at VNIIEF to consider the applicability of unstructured Lagrange meshes to multidimensional continuum mechanics problems with high shear strain and vortex flows. Three finite-difference numerical techniques for solving continuum mechanics problems on polyhedral unstructured Lagrange meshes are described. Examples of numerical calculations of benchmark problems are given.

Introduction

Finite-difference methods have gained broad application in numerical computations of time-dependent continuum mechanics problems. As early as in the mid-1950s, pioneering techniques were developed to provide numerical calculations of 2D gas dynamics problems. With the advancement of computer engineering, there also started to emerge numerical modeling techniques for 3D flows, being a generalization of 2D techniques to 3D cases. Numerical techniques for 2D continuum flow simulation mainly use structured tatragonal meshes, and for 3D flows, structured hexahedral meshes. At that, problems with small strain in materials are usually solved on Lagrange meshes, whereas those with high shear strain and stream flows are solved on Eulerian or Lagrange-Eulerian meshes. The wider use of structured meshes as applied to continuum mechanics problems is attributed to their rather high efficiency and simplicity of computational algorithms.

The development of unstructured mesh techniques at VNIIEF was initiated in the mid-1960s by I.D.Sofronov, who pointed at the utility of such an approach (Sofronov, 1966). Meshes comprised of arbitrary polygons and polyhedrons remove a number of difficulties in generating the initial mesh, which are typical of structured meshes, significantly simplifying the generation of initial meshes with specified parameters in complex-geometry domains. Unstructured mesh techniques allow local mesh reconfiguration tools to be used both to change the number of points and to change the number of point sets. This extends computational capabilities as applied to high shear strains in Lagrange variables. Therefore, it is more reasonable to use unstructured mesh techniques for solving complex-geometry problems, which are poorly described by structured meshes, problems with high shear strain and stream flows. In addition, the accuracy of computations in Lagrange variables is generally higher than in computations

with the same number of points but in Eulerian variables. Techniques for solving continuum mechanics problems on unstructured meshes are developed at VNIIEF by different teams in two directions – using Lagrange and free Lagrange methods. Unstructured polygonal meshes underlie the DMK and MEDUZA techniques (Sofronov et al., 1984), which were originally intended for 2D gas dynamics problems and then incorporated heat conductivity (Panov, 2004), elastoplasticity (Sokolov, 2004) and magnetohydrodynamics. In 1987, I.D.Sofronov and V.V.Rasskazova suggested generalizing the 2D Lagrange technique DMK to a 3D case, which resulted in the TMK technique (Rasskazova, Sofronov, 1987, Rasskazova et al., 1998). The free Lagrange technique MEDUZA was generalized to 3D gas dynamics problems on unstructured meshes in MEDUZA-3D (Butnev et al., 2003).

Problem Definition

Let us consider two equations of motion of isotropic continuum:

$$\begin{cases} \dfrac{d\rho}{dt} = -\rho \operatorname{div} \vec{u}; \\ \rho \dfrac{d\vec{u}}{dt} = -\operatorname{grad} P + \operatorname{div} S + \dfrac{1}{4\pi}\left[\operatorname{rot} \vec{H} \times \vec{H}\right]; \\ \dfrac{d}{dt}\left(\dfrac{\vec{H}}{\rho}\right) = \left(\dfrac{\vec{H}}{\rho} \cdot \vec{\nabla}\right)\vec{u} \\ \dfrac{dE}{dt} = -P\dfrac{d}{dt}\left(\dfrac{1}{\rho}\right) + \dfrac{1}{\rho} S_p\left(SD\right) + \dfrac{1}{\rho}\operatorname{div}(\kappa \operatorname{grad} T); \\ \dfrac{d\vec{r}}{dt} = \vec{u}, \end{cases} \tag{1}$$

where ρ is the matter density, E is the specific internal energy, T - the temperature, κ - the heat conductivity factor, $\vec{u} = (u, v, w)$ - the velocity vector, $\vec{r} = (x, y, z)$ - the radius vector, P - the pressure, S - the strain tensor deviator, D - the strain rate tensor, $S_p(SD)$ - the first invariant of tensor SD, and $\vec{H}$ is the magnetic field strength vector .

To close the system of differential equations, let us use the equation of state of the matter: $P = P^{\Gamma}\left(\rho, E\right)$. (2)

If the matter is described by a gas dynamics model, $S = 0$. If the medium is described by an elastoplastic model, $S = S^{\text{уп}}$; $P = P^{\text{г}}$. In this case, in order to define the deviator component of the strain tensor, let us use the Hooke law in the differential form:

$$\frac{\delta S^{\text{уп}}}{\delta t} = 2G\left(D - \frac{1}{3} S_p D\right) \tag{3}$$

where G is the shear modulus, and $\dfrac{\delta}{\delta t}$ is the time derivative along the moving direction.

In the region of plastic strain, let us use the Mises flow rule to correct the strain tensor deviator: $\dfrac{3}{2} S_{ij}^{\text{уп}} S_{ij}^{\text{уп}} = Y^2$, (4)

where Y is the yield stress, which can be a constant (for an ideal plastic matter) or a function (for materials with hardening).

If the material is described by an elastoviscoplastic model, then:

$$P = P^{\text{г}} + P^{\text{в}}\,;\; S = S^{\text{уп}} + S^{\text{в}}\,,\;\; P^{\text{в}} = \frac{1}{3}\mu_1 S_P D\,;\; S^{\text{в}} = \mu_2\left(D - \frac{1}{3}S_P D\right); \tag{5}$$

where $P^{\text{г}}$ is derived from Eq. (2); $S^{\text{уп}}$ is derived from Eqs. (3), (4); $P^{\text{в}}, S^{\text{в}}$ are the viscous pressure and the strain tensor deviator; and μ_1, μ_2 are the values of dynamic viscosity.

Major Features of the TMK Technique

The first 3D technique to solve 3D gas dynamics problems on unstructured polyhedral Lagrange meshes was TMK, a technique developed under the guidance of I.D.Sofronov and V.V.Rasskazova (Rasskazova and Sofronov, 1987, Rasskazova et al., 1998). This technique was further extended to time-dependent elastoplastic flows (Sokolov, 2002). For solving gas dynamics and elastoplasticity difference equations, the technique uses an explicit difference scheme, which allows velocities to be specified at mesh nodes, and density, energy, pressure and strain, in mesh cells. In generating a finite-difference scheme, one uses a spaced-apart centering template: kinematic values are set at difference mesh nodes, and thermodynamic, in cell centers. In order to define mesh node velocities, one uses the integral representation of the law of conservation of momentum integrated over the space embracing the node from the side of four adjacent cells. The mesh is defined by arbitrary convex polyhedrons (Fig.1a).

The space is filled by figures without folds and gaps irregularly, but one condition should necessarily be met – there should be no more than four cells converging in any mesh node. This condition can always be met if Dirichlet cells or Voronoi figures are used as convex polyhedrons at the initial point of integration time. The mesh is defined by coordinates and mesh node connections using coordinates of cell centers at the stage of initial Dirichlet mesh generation. Each mesh node adjoins four nodes and four mesh cells. Each node's connections are organized. With minimum mesh information, one can always obtain any data required (determine the quantity and the numbers of mesh nodes comprising the face partitioning these cells; determine the numbers of all adjacent cells). The Dirichlet mesh generation algorithm is of recurrent nature. In N steps, one obtains a finished Dirichlet mesh composed of N cells (Fig.1.b). At the initial point of time, the mesh consists of convex polyhedrons with plane faces.

In order to maintain the mesh in good condition in running a problem, one uses the method of elastic impact developed by V.V.Rasskazova (Rasskazova et al., 1998), which keeps trihedral angles convex with respect to the figure center over integration time, and the local polyhedral cell reconstruction technique. TMK is intended for numerical solution of single-domain 3D gas dynamics and elastoplasticity problems on unstructured polyhedral meshes with a fixed neighborhood structure.

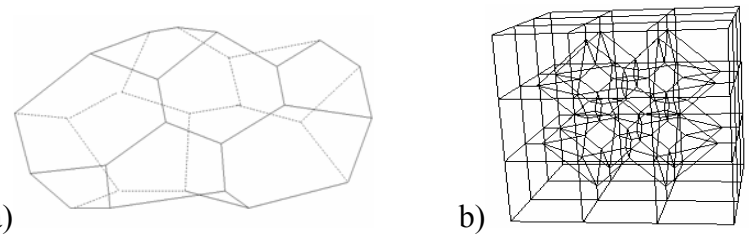

Figure 1 - A 3D mesh cell a) and the Dirichlet mesh contained in a cube – b).

Major Features of the MEDUZA-3D Technique

The major features of the free-Lagrange technique MEDUZA-3D (Butnev et al., 2003) are the use of an unstructured mesh, centering of all gas dynamics values on the node, variable difference template for the numerical integration of differential equations and the possibility to change the mesh topology in running a problem. Boundaries are described by mixed cells calculated by the lumping method. The technique for solving 3D gas dynamics problems on unstructured meshes is a generalization of the MEDUZA-2D technique (Sofronov et al., 1984) for 2D problems.

System (1) for the gas dynamics case is sought within the problem domain with specified initial and boundary conditions. One considers a set of points (mesh nodes), to which all thermodynamic and kinematic functions are assigned. The initial point distribution is set based on the initial and boundary conditions of the problem and a priori considerations of the problem solution. For each point, one defines a set of its neighbors based on the Euclidean metric. The neighborhood is defined using a tetrahedration process. The point set with the defined neighborhood generates the mesh. The technique uses a single-domain problem solution model. This produces mixed cells at interfaces, whose solutions are sought based on the multi-component approach. Mesh cells are polyhedrons with mesh nodes inside; all kinematic and thermodynamic values are centered on nodes.

The cell construction algorithm rests upon the attraction of tetrahedron gravity centers, tetrahedron face gravity centers and edge centers. Mesh topology is stored using an approach, in which a point refers to an arbitrary adjoining tetrahedron, and each tetrahedron refers to four tetrahedrons adjacent to it and four of its vertices. The use of tetrahedrons made it possible to solve the problem of partitioning the interface in a mixed cell, if the node itself and its neighbors lie on the Lagrange surface. In this case, by assigning a material property to each tetrahedron at the initial stage, we will keep the tetrahedrons "pure" unless a point is shifted (moved apart) or the mesh is restructured to produce mixed tetrahedrons. In a 3D case, the integration of the equation of motion comes down to the solution of the surface integral $\iint_{\Delta}(P+q)\vec{n}dS$, where P, q are the material and viscous pressures, $\vec{n}$ is the outer normal vector, dS is the triangle area, Δ are all the triangles making the surface of the integration cell. As shown in Fig. 2a, each face of the integration cell is a triangle (for definiteness, let us consider the triangle OId, whose vertices are the centers of the tetrahedron O and one of the faces of the tetrahedron I and the middle of one of the edges of the tetrahedron d). Let us define the values of pressure at these points using linear combinations of values at tetrahedron vertices 1,2,3,4. Following this, the value of total pressure is defined as an arithmetic mean of the

values of total pressures at the triangle vertices:

$$(P+Q)_{Old} = \frac{13(P+q)_1 + 2(P+q)_2 + 13(P+q)_3 + 7(P+q)_4}{36} \quad (6)$$

If a corresponding face of the integration cell lies at a boundary with a specified boundary pressure, the value of pressure at the boundary is not calculated using the above procedure, but is taken directly from the boundary condition. The sum vector of the force acting upon the cell is calculated by summing up elementary forces acting upon the elementary triangles of each tetrahedron with a respective sign.

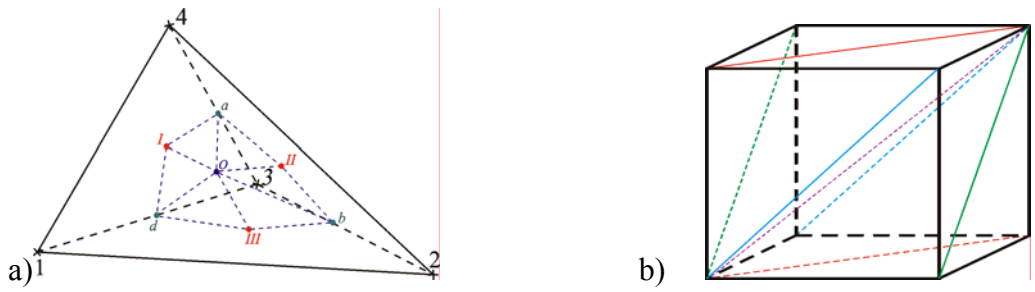

Figure 2 – Six triangles of the integration surface related to node 3 – a); tetrahedration of a hexahedron – b)

The initial unstructured mesh is derived from a structured hexahedral one by splitting each hexahedron into six tetrahedrons. Fig. 2b) shows an example of the tetrahedration of a hexahedron. In order to suppress high-frequency perturbations, one uses the velocity field smoothing operator $O(\tau \cdot h^3)$.

Major Features of the TIM Technique

The TIM technique (Sokolov et al., 2004) serves for 3D continuum mechanics computations on polyhedral unstructured Lagrange meshes. It allows computations to be performed on meshes with an arbitrary number of node connections (number of adjoining cells). The technique is also valid both on the Dirichlet-Voronoi unstructured polyhedral meshes, and on hexahedral meshes and unstructured polyhedral meshes having an arbitrary number of neighborhoods in a node. The technique uses the same computational algorithm for all the meshes. Initial data and continuum mechanics equations are calculated in Cartesian coordinates. The technique is intended for solving gas dynamics, time-dependent elastoplasticity, magnetohydrodynamics and heat conductivity problems.

Let us seek solution to a problem stated in Cartesian coordinates (x, y, z) in a given domain V bounded by the surface C on the assumption that all necessary initial and boundary data are specified. In generating a finite-difference scheme for solving system of differential equations (1), one uses the integro-interpolation process assuming that:

1) the values $P, \rho, E, q, S_{ij}, \dot{\varepsilon}_{ij}, \vec{H}, T$ are assigned to the centers of polyhedrons (cells) and are constant within them;
2) the values x, y, z are assigned to the vertices of polyhedrons (nodes);
3) the values u, v, w are assigned to the vertices of polyhedrons and are constant within the volumes related to the nodes;
4) faces are described by their piecewise linear representation.

To calculate the cell volume, let us consider a computational cell comprised of N vertices (nodes). At distortions, the cell's faces, being polyhedrons in space, may be non-planar. To this end, the cell is split up into a system of tetrahedrons, each having vertices in the center of the computational cell, in the center of the face and at two neighbor vertices of this face. The cell volume is defined as a total of the volumes of these tetrahedrons. The mass of nodes is defined as a total of mass shares (per vertex) of the cells converging in the node. In running a problem, node masses and cell masses are constant.

In solving time-dependent gas dynamics and elastoplasticity problems (Sokolov, 2002), one uses a fully conservative explicit difference scheme. As applied to structured meshes, it has the second order of accuracy in space and time. As artificial viscosity one uses a combination of the quadratic and linear viscosity. The velocities of mesh nodes are defined using the law of conservation of momentum in the integral form. The integration is performed over the volume V embracing the node from the side of the cells adjoining the node bounded by the surface C using the Gauss-Ostrogradsky formula:

$$\iiint_V \rho \frac{du}{dt} dV = \iiint_V \left(-\frac{\partial(P+q)}{\partial x} + \frac{\partial S_{xx}}{\partial x} + \frac{\partial S_{xy}}{\partial y} + \frac{\partial S_{xz}}{\partial y} \right) dV = \iint_C \left(-(P+q)\vec{i} + S_{xx}\vec{i} + S_{xy}\vec{j} + S_{xz}k \right) \vec{n} dC \qquad (7)$$

$$\iiint_V \rho \frac{dv}{dt} dV = \iint_C \left(S_{xy}\vec{i} + (S_{yy} - P - q)\vec{j} + S_{yz}\vec{k} \right) \vec{n} dC; \quad \iiint_V \rho \frac{dw}{dt} dV = \iint_C (S_{xz}\vec{i} + S_{yz}\vec{j} + (S_{zz} - P - q)\vec{k}) \vec{n} dC,$$

where $\vec{i}, \vec{j}, \vec{k}$ are the coordinate unit vectors, $\vec{n}$ is the normal to the surface C.

In solving magnetohydrodynamics problems with a frozen-in field, the magnetic field strength vector is defined in the centers of mesh cells, and the current density and electromagnetic force vectors are assigned to mesh nodes. We use a fully conservative explicit difference scheme. For solving the magnetic induction equation, we integrate it over the computational cell Ω. Let the cell volume be V. By integrating both members of the equation over Ω, we obtain the equation:

$$\frac{d\left(\vec{H}V\right)}{dt} \approx H_x \int_{\partial\Omega} \vec{u} dydz + H_y \int_{\partial\Omega} \vec{u} dzdx + H_z \int_{\partial\Omega} \vec{u} dxdy \qquad (8)$$

The integrals in the right-hand member of this equation are substituted by finite sums.

In solving a heat conductivity equation, the value of temperature is defined in cell centers, and the heat flow vector, at the nodes. The difference scheme is constructed using the process of generalized derivation of discontinuous functions and is implicit and conservative (Panov, 2004). The approximation of the differential operator in the heat conductivity equation on structured meshes has the second order of accuracy in space. The resulting difference system of linear equations has a symmetric and positively definite matrix. The system of equations is solved by the iteration method of conjugate gradients using different types of preconditioners, as the incomplete Cholesky decomposition, the Schwartz decomposition method, etc.

Types of initial meshes used in the TIM technique

The technique uses the following types of initial computational meshes:

- unstructured polyhedral mesh composed of Dirichlet cells or Voronoi figures (with the inside angle surrounding four cells) – Fig.3.a.
- unstructured polyhedral mesh derived from a 2D unstructured mesh – Fig. 3 b-c. It can be generated by rotating a 2D mesh around the axis or by shifting a sheet with a 2D mesh in space. Internal nodes of the mesh are convergence points of six cells.
- Hexahedral mesh (described by an irregular structure with an arbitrary neighbor connectivity) – Fig. 3d. Internal nodes of the mesh are convergence points of eight cells.

An initial mesh for solving complex-geometry problems may comprise several types of meshes (for example, hexahedral and polyhedral) in a single domain at once – Fig.4.

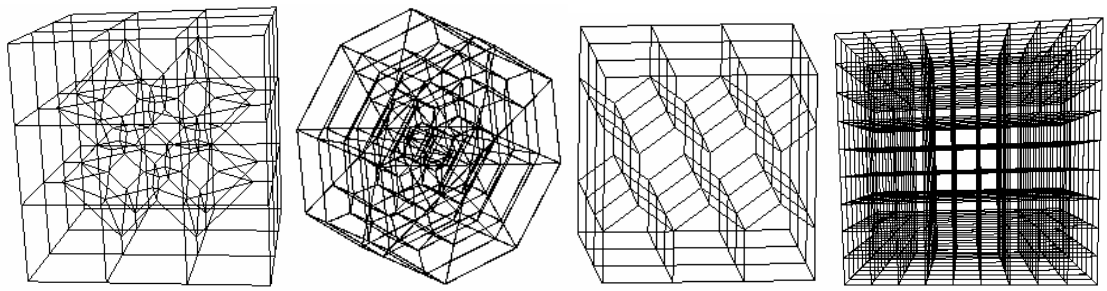

a) b) c) d)

Figure 3 – The Dirichlet-Voronoi mesh - a); unstructured meshes derived from a 2D mesh - b) and c); a hexahedral mesh - d)

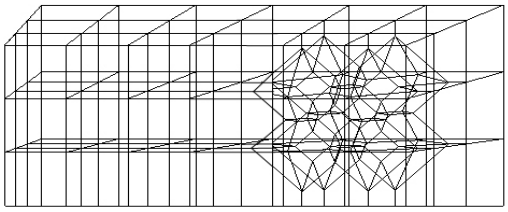

Figure 4 – Example of a mesh having hexahedral and Dirichlet-Voronoi cells in one domain

Mesh maintenance in the TIM technique

Mesh maintenance is known to be one of the problems encountered in numerical calculations using high-strain Lagrange techniques. TIM provides special mesh maintenance methods, which can be used concurrently with numerical calculations in any combination.

Method 1. In most techniques, mesh adjustment is subject to a restriction that computational cells should be convex. The cell convexity condition is a considerable constraint for meshes, especially for 3D hexahedrons. This condition is excessive if the mesh should be maintained such as to have no overlaps. Tolerating non-convex cells may considerably enhance capabilities for initial mesh calculation algorithms. It should be noted here that an acceptable mesh is understood to be a mesh having no self-intersecting cells. Cell faces are space polygons, which are non-planar figures. Mesh maintenance is performed by imposition of differentiable connections, which implements a number of mesh maintenance algorithms (see Fig. 5):

- meshes containing “stellar” cells (all cell nodes are located in the line of sight from the cell center);
- meshes with convex dihedral cell angles (the dihedral angle is made by two faces of the cell with a common edge);
- meshes with convex polyhedral cell angles (the polyhedral angle is made by cell edges meeting in one node).

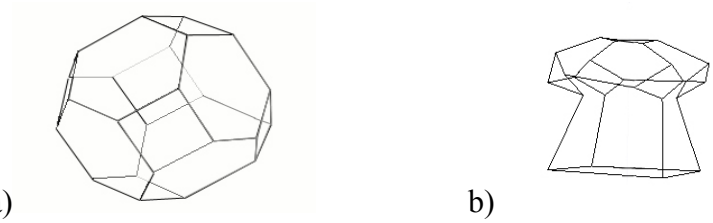

Figure 5 – Convex cell – a); non-convex “stellar” cell - b)

Method 2. In calculating problems with high shear strain, vortex and stream flows, cells may stretch in any direction, which distorts the approximation of solution, or get strongly compressed, which reduces the mesh dimension. In order to more successfully use the technique in numerical experiments, it is equipped with local adjustment tools for polyhedral meshes. At that, after performing the local mesh adjustment, an arbitrary number of cells may meet in a node. Local adjustments of 3D meshes rest upon two operations – partitioning and integration of cells.

Method 3 is based upon the process of velocity field smoothing in mesh nodes to suppress high-frequency perturbations. It provides smoother solutions and enhances the mesh quality by reducing the work load on the algorithms implementing the two above methods.

Calculations of multi-domain problems using the TIM technique

In calculating complex 3D problems, the system’s initial geometry often needs to be divided into domains. Such a division is often necessary for a more accurate description of interacting solids with assigned slide planes (boundary). In running a problem, the faces of polyhedral cells (including boundary cells) are non-planar figures. Therefore, in order to solve the problem of contact interaction at the interface of two media, one first triangulates the two interacting surfaces (an additional triangular mesh is introduced). The triangulation of the interface using the additional mesh is performed from the centers of boundary cells towards its nodes. In order to calculate the contact interaction, all necessary kinematic values are converted to the additional mesh.

Examples of Calculations

Decay of an arbitrary discontinuity in gas dynamics settings

Let us consider numerical calculations of the problem of arbitrary discontinuity decay. Let an ideal gas, whose conditions are defined as follows: left – $\rho_I = 1;\ P_I = 2.5;\ u_I = 0$, right $\rho_{II} = 1;\ P_{II} = 0.5;\ u_{II} = -2.8026$, at the initial point of time $t = 0$ be situated to the left and to the right of the plane $x = 0.5$. The adiabatic index is $\gamma = 1.4$. All surfaces of the domain are “rigid walls”. The comparison of the numerical

solution to the problem obtained by means of TIM using different number of points along the direction of shock propagation with an analytical solution for the point of time $t = 0.24$ is shown in Fig. 6.

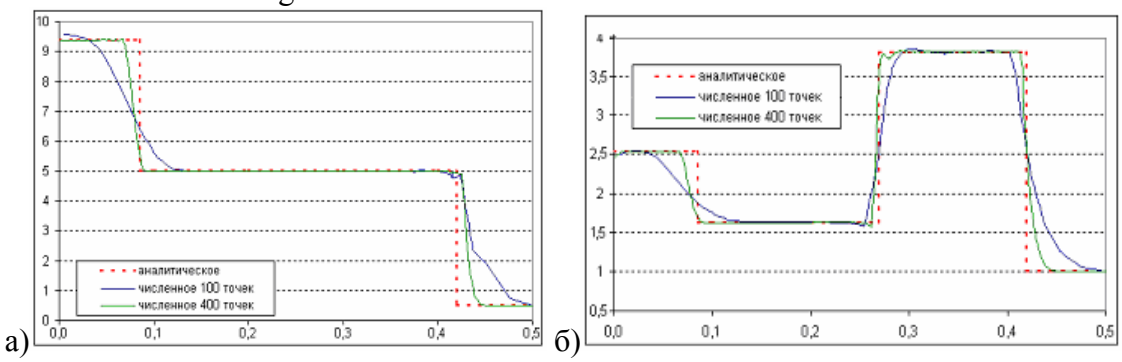

Figure 6 – Pressure distribution - a) and density - b) at $t = 0.24$

The plane stress wave problem

Let us consider a plane elastoplastic problem of half-space deformation having an accurate solution. The initial geometry is a rectangular bar with the following dimensions: $|AB| = 1,5cm$, $|AA'| = |AD| = 0,5cm$. The number of specified points in the problem is 1,200. Initial conditions: $\rho_0 = 1$ g/cm^3, $\vec{u} = 0$, $E_0 = P_0 = S_{x_i x_i} = 0$. The material is described by the equation of state $P = (\gamma - 1)\rho E$ with an adiabatic index $\gamma = 3$ and by an ideal elastoplastic model. Elastoplastic properties of the material: $G = 15$ GPa, $Y_0 = 1$ GPa. Time-independent pressure $P_{\text{гр}} = 5$ GPa is specified on the left boundary; all other boundaries are rigid walls. The calculations were performed using the TIM code. Figs.7.a – 7.c show the results of numerical calculations and analytical solution for $t = 2.4$ μs. The calculations resulted in the break-up of the shock wave into two parts: an elastic front wave traveling at a velocity $D_{\text{elastic}} = 4,52$ km/s is followed by a plastic wave $D_{\text{plastic}} = 3,26$ km/s. The results of the calculations are in good agreement with the analytical solution ($D_{\text{elastic}} = 4,5$ km/s, $D_{\text{plastic}} = 3,25$ km/s).

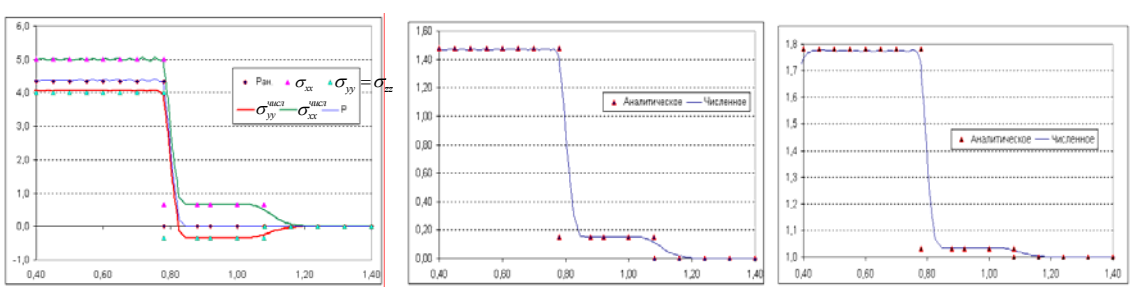

a) *b)* *c)*

Figure 7 – The plane stress wave problem: a*)* pressure and stress profiles; b*)* velocity profiles; c*)* density distribution profiles

The Richtmyer-Meshkov instability growth problem

The domain with dimensions 0≤X≤12cm, 0≤Y≤12cm, 0≤Z≤24 cm is occupied by Freon and air. Freon-occupied domain size is 0≤X≤6cm, 0≤Y≤6cm, 0≤Z≤9 cm. Constant velocity $\vec{\mathbf{U}} = (0,0,-21.056456$ cm/ms) is assigned to the upper boundary. Air pressure is

P_1=1 atm, and density is ρ_1=0.001205 g/cm^3. In Freon, P_2=1 atm, density ρ_2 = 0.00513 g/cm^3. The equation of state of the matter is given by an ideal gas with γ_1=1.4 for the air, and γ_2=1.139 for Freon. The calculations were carried out using the MEDUZA-3D code. Fig. 8 illustrates the results of the calculations for **t**=0.764 ms and shows the shape of Freon and the pressure field.

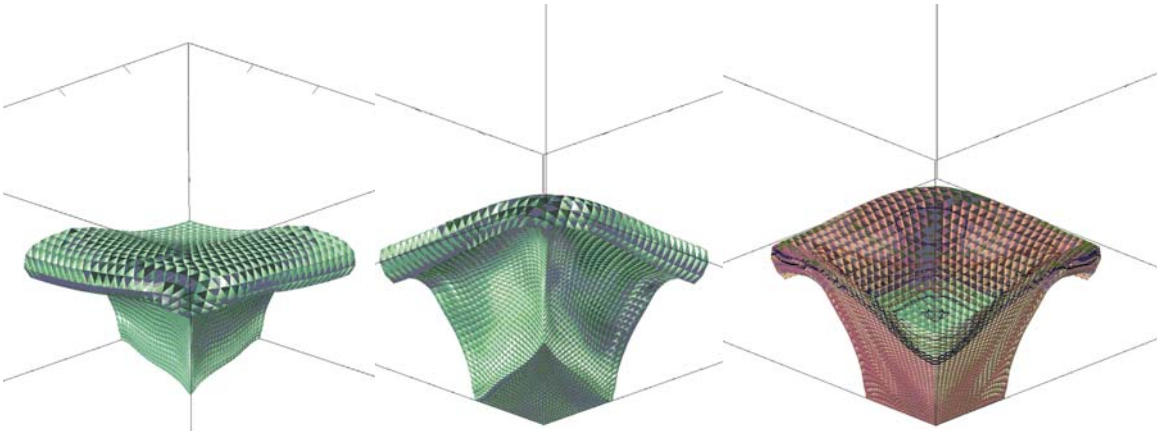

Figure 8 – The shape of Freon and the pressure field for the point of time **t=0.764 ms**

The problem of bar impact against a wall

As applied to high-strain problems, the TMK and TIM techniques were validated using the problem of a bar penetrating into a wall in the gas dynamics and elastoplastic approximations.

Gas dynamics simulation. The projectile and wall materials were described by the equation of state of an ideal gas with $\gamma = 1.4$. In this problem, the projectile has a configuration of a 2 x 2 x 10-cm parallelepiped, which flies at a velocity of 10 km/s and collides with a solid in the form of a cube having a 10-cm edge. Initial density is $\rho_0 = 1$ g/cm^3 , pressure and energy are taken as zero. The projectile's edges are defined as "free boundaries"; and all wall edges, except the colliding one, are defined as "rigid walls". The calculations were carried out using the TMK and TIM codes on the Dirichlet-Voronoi Lagrange mesh having 31,400 computational cells.

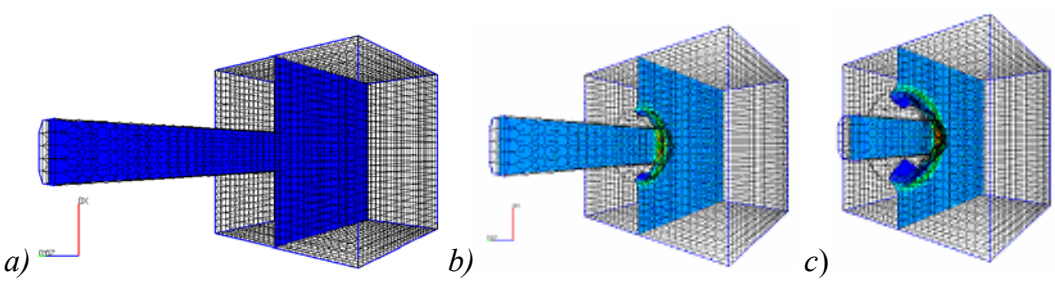

Figure 9 – Projectile penetration into a wall, gas dynamics:
a) initial geometry; *b)* t =3.5 μsec; *c)* t =7 μsec

Fig. 9 shows the initial geometry of the problem and dynamics of projectile embedding into a wall with the computational mesh and section by the Oxz plane; color fill visualizes the matter density.

Elastoplastic simulation. The materials of the projectile and the impacted solid were defined as steel. Steel was described by the Mie-Gruneisen equation of state and the model of ideal elastoplasticity having the following parameters: $\rho_0 = 7.8$ g/cm^3; $c_0 = 4.9$ km/s; $n = 5$; Γ=1.66; $\sigma_s = -2.5$ GPa; $G = 81$ GPa; $Y = 1.05$ GPa. The initial 3D mesh, dimensions and configuration of the projectile and the wall are the same as in the above simulation. The projectile travels at a velocity of 1 km/s. Initial density is $\rho_0 = 7.8$ g/cm^3, pressure and energy are equal to zero. The projectile's edges are defined as "free boundaries"; and all wall edges, except the colliding one, are defined as "rigid walls". The calculations were carried out for the point of time 40 μsec using the TMK and TIM codes. Fig. 10 shows the dynamics of projectile embedding into a wall with the computational mesh and section by the Oxz plane; color fill visualizes the matter density.

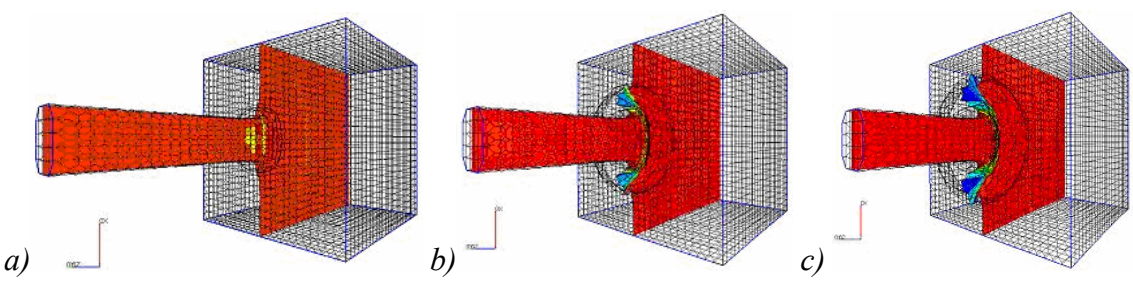

Figure 10 – Dynamics of projectile penetration into a wall, elastoplasticity: *a)* $t = 10$ μsec; *b)* $t = 30$ μsec; *c)* $t = 40$ μsec

The ellipsoid compression problem

The "crash-free" property of the techniques as applied to high-strain problems was tested by solving the ellipsoid compression problem using the velocity field smoothing algorithm. At the initial point of time $t = 0$, the computational domain is an ellipsoid with semi-axes $a = 1.5$; $b = 1.5$; $c = 1$. The ellipsoid contains a uniform resting ideal gas described by the equation of state $P = (\gamma - 1)\rho E$, density $\rho = 200$, $\gamma = 1.3333$. At the initial point of time, the ellipsoid gets compressed by constant pressure, varying with time according to the law: $P(t) = t$ for 0<t<5, $P(t) = 5$ for $t \geq 5$. The calculations were carried out using the TIM code on a hexahedral (8,000 points) and polyhedral (22,575 points) mesh. Fig. 11 shows the configurations of the computational domains for $t = 9.0$, $t = 15.0$ and $t = 20.0$ with pressure distribution in the OXY section for the hexahedral (Fig. 11a) and polyhedral (11b) mesh. At $t = 9.0$, the ellipsoid has a shape of a disk; at $t = 15.0$, its shape is close to the domain. By $t = 20.0$, the ellipsoid stretches and flattens. The behavior of the ellipsoid in these calculations is qualitatively the same. Note that the problem was calculated crash-free up to the point of time $t = 50.0$.

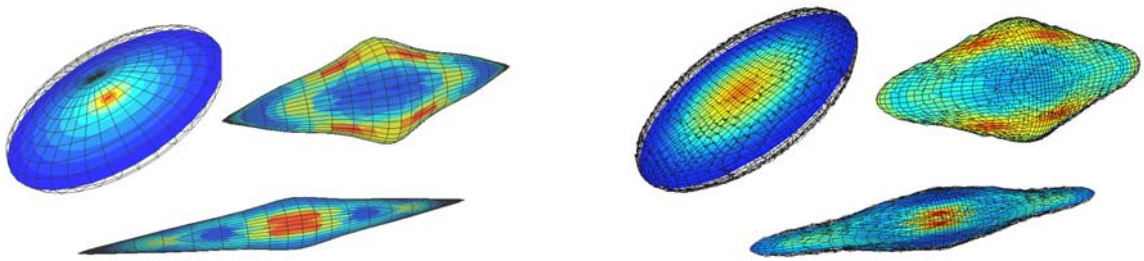

a) b)

Figure 11 – Ellipsoid compression dynamics with mesh mapping in the OXY section

The cooling cube problem

Cooling cube simulation was performed to validate the TIM technique as applied to the diffusion equation. The problem's diffusion equation is: $\frac{\partial T}{\partial t} = \frac{\partial^2 T}{\partial x^2} + \frac{\partial^2 T}{\partial y^2} + \frac{\partial^2 T}{\partial z^2}$. The computational domain is a $[0,1]\times[0,1]\times[0,1]$ cube. The initial temperature specified within the cube is $T = 1$, and the temperature at its boundary is $T = 0$. The analytical solution to the problem takes the following form:

$$T(x,y,z,t) = f(x,t)f(y,t)f(z,t),\ f(x,t) = 4\sum_{k=0}^{\infty}\frac{\exp\left(-\pi^2(2k+1)^2 t\right)}{\pi(2k+1)}\sin\left(\pi(2k+1)x\right) \quad (9)$$

The problem was calculated on a hexahedral mesh with a time step of 0.0005. The mesh had 20 cells in each direction. Fig. 12 shows the comparison of analytical solution over calculations for $t = 0.05$. In order to compare the analytical and the numerical solution, points with coordinates $\left(T_a^i, T_c^i\right)$ were plotted for all i-th cells, where T_a^i, T_c^i are the analytical and numerical values of temperature in the i-th cell. The comparison of the numerical and the analytical solution proves that calculations are reasonably accurate.

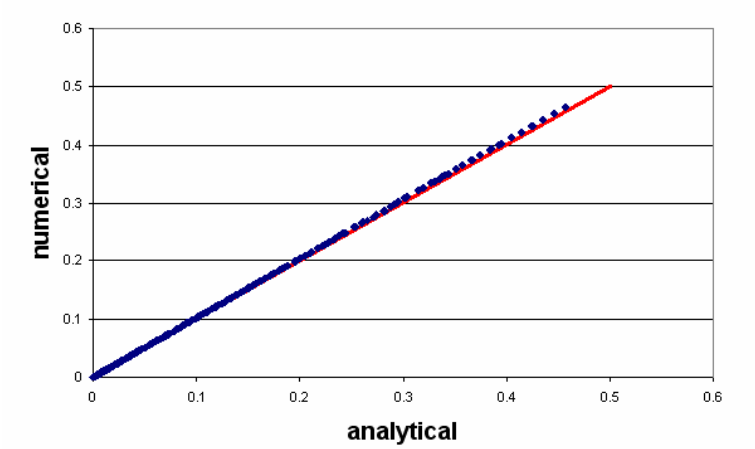

Figure 12 – Analytical vs. numerical solution for $t = 0.05$

Problem of a spherical piston in a dipole magnetic field

The problem's geometry is a spherical enclosure with an inside sphere of initial radius R_0 expanding at a constant rate u_R. The domain is defined as a dipole magnetic field with axis orientation along the x-axis and radius R_0:

$$H_x = H_0\left(1+\frac{1}{2}\left(\frac{R_0}{R}\right)^3-\frac{3}{2}\left(\frac{R_0}{R}\right)^3\left(\frac{x}{R}\right)^2\right), \qquad H_r = -H_0\cdot\frac{3}{2}\left(\frac{R_0}{R}\right)^3\left(\frac{rx}{R^2}\right), \qquad (10)$$

where $r^2 = y^2+z^2$, $R^2 = x^2+y^2+z^2$. If $H_0 \gg u_R$ (strong magnetic field), the approximate analytical solution to the problem would be a dipole magnetic field with radius $R_0(t) = R_0 + u_R t$. The calculations were performed on a mesh generated by rotating a 2D mesh around the OX axis. The 2D mesh had 40 cells in the radial direction, and 80 cells in the angular direction. The 3D mesh consisted of three "layers". The radius of the inner sphere R_0 is 0.5; the radius of the outer sphere is 3. Piston velocity is $u_R = 0.1$, magnetic field strength is $H_0 = 5$. The matter is assumed to be an ideal gas with adiabatic index $\gamma = 2$ and initial density $\rho_0 = 1$. The calculations were carried out using the TIM code. To compare the analytical and numerical solution, analytical and numerical values of the magnetic field strength vector component (H_i^{an} and H_i^{num}, respectively) were considered for each i-th cell. Fig. 13 shows points with coordinates $\left(H_i^{an}, H_i^{num}\right)$ for all i-th cells and their position with respect to the line $y=x$. The comparison of the analytical solution with the calculations shows that the latter are reasonably accurate.

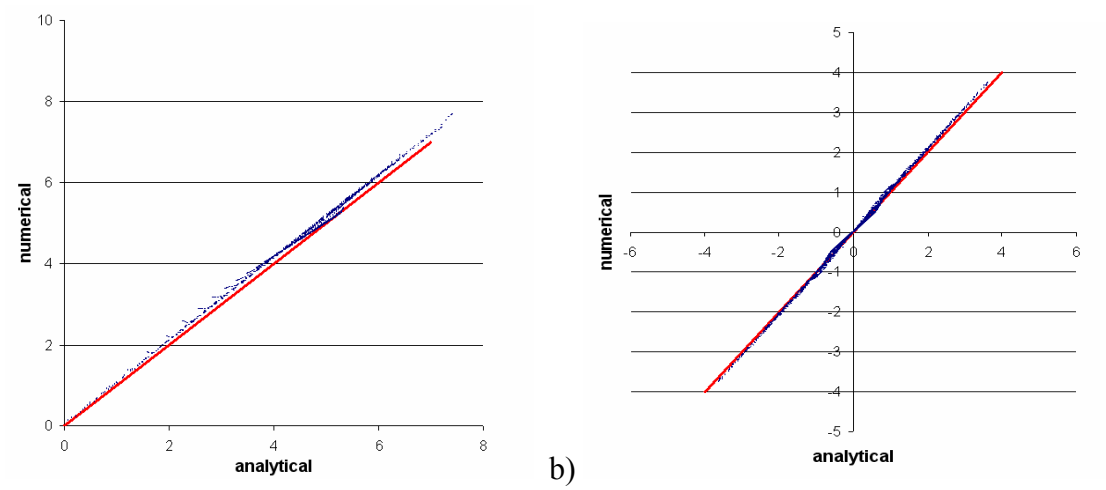

a) b)

Figure 13 – Values of H_x - a) and H_r - b) at the point of time $t = 0.31$

Conclusion

This paper provides an overview of three techniques developed at VNIIEF to solve 3D continuum mechanics problems on unstructured polyhedral meshes. Their development was facilitated by the wide practical experience gained at VNIIEF in using

the Lagrange technique DMK and the free Lagrange technique MEDUZA for solving 2D continuum mechanics problems on unstructured polygonal meshes. The practical interest to the application of unstructured meshes is particularly clear, when these are used for solving complex-geometry problems with local small-scale sub-domains, in which the use of polygonal and polyhedral cells allows generating meshes with specified properties in a more efficient way. The results of the benchmark problem calculations on polyhedral unstructured Lagrange meshes demonstrated their validity.

References

Sofronov I.D. Numerical calculations of a heat conductivity equation on a non-orthogonal mesh (in Russian) // Proceedings of the 1st International Congress of Mathematicians. Section 14, Moscow, 1966

Sofronov I.D., Rasskazova V.V., Nesterenko L.V. The use of nonregular nest for solving two-dimension nonstationary problems in gas dynamics // Numerical Methods in Fluid Dynamics. M.: Mir Publishers, 1984. P. 82-121.

Rasskazova V.V., Sofronov I.D.. Some aspects of numerical calculations of 3D continuum mechanics problems (in Russian) // Voprosy Atomnoi Nauki i Tekhniki (VANT). Series: Technique and codes for numerical simulation of mathematical physics problems. 1987. Issue 1. P. 44-57.

Rasskazova V.V., Sofronov I.D., Eremenko A.Yu., Motlokhov V.N. A technique for solving 3D time-dependent gas dynamics problems on unstructured Lagrange meshes (in Russian) // Voprosy Atomnoi Nauki i Tekhniki (VANT). Series: Mathematical modeling of physical processes. Issue 4. 1998. P.44-57.

Butnev O.I., Barabanov R.A., Volkov S.G., Zhogov B.M., Pronin V.A. MEDUZA-3D code for solving 3D gas dynamics problems on unstructured meshes. Richtmyer-Meshkov instability simulations (in Russian). // Youth in Science. Proceedings of the 2nd Scientific Conference. Sarov. 2003. P.13-18.

Sokolov S.S. A technique for solving time-dependent elastoplastic problems on unstructured polyhedral Lagrange meshes (in Russian)// Voprosy Atomnoi Nauki i Tekhniki (VANT). Series: Mathematical modeling of physical processes. 2002. Issue 4. P.23-36.

Sokolov S.S. A method for solving 2D time-dependent elastoplastic flows on unstructured polygonal Lagrange meshes (in Russian) // Voprosy Atomnoi Nauki i Tekhniki (VANT). Series: Mathematical modeling of physical processes. 2004. Issue 4. P.62-80.

Panov A.I. A technique for solving a heat conductivity equation on unstructured meshes (in Russian) // Voprosy Atomnoi Nauki i Tekhniki (VANT). Series: Mathematical modeling of physical processes. 2004. Issue 4. P. 27-40.

Sokolov S.S., Panov A.I., Motlokhov V.N., Voropinov A.A., Novikov I.G., Sobolev I.V., Yalozo A.V. The TIM technique for 3D flow simulation on unstructured polyhedral Lagrange meshes with an arbitrary number of node connections (in Russian) //Proceedings of the International Workshop on Supercomputations and Mathematical Modeling. Sarov, 2004.